Small-Signal Analysis and Design of Weighted Voltage-Mode Control for a Multiple-Output Forward Converter

Qing Chen and Fred C. Lee
Virginia Power Electronics Center
The Bradley Department of Electrical Engineering
Virginia Polytechnic Institute and State University
Blacksburg, VA 24061

Milan M. Jovanović
DELTA Power Electronics Lab., Inc.
1861 Pratt Drive
Blacksburg, VA 24060

Abstract *- The small-signal model for a multiple-output forward converter with weighted voltage-mode control is derived. The effects of the weighting factors on the small-signal behavior are investigated. In addition, the small-signal characteristics of weighted voltage-mode control are compared with the characteristics of a multiple-output converter with coupled output-filter inductors. Finally, the effects of weighted voltage-mode control on the small-signal characteristics of the converter with coupled inductors are examined. Based on the analysis, the design procedure for loop compensation is presented. The small-signal model and the design procedure are verified on an experimental two-output forward converter.*

I. INTRODUCTION

The most common approach to regulate multiple-output converters is to sense one output while cross-regulating the remaining outputs. This regulation scheme provides tight regulation for the sensed output. The cross-regulated outputs, however, may severely deviate from the desired values, especially during the transients due to step load changes [1-3]. The transient characteristics of the cross-regulated outputs can be improved dramatically by coupling the output filter inductors [4]. While this approach improves the dynamic behavior of the cross-regulated outputs, it does not have significant effect on their dc cross-regulation characteristics [5,6,7].

Simultaneous improvements of the transient and dc performance of the cross-regulated outputs can be obtained by using weighted voltage-mode control (WVMC) [8,9]. In this approach, shown in Fig. 1, a number of outputs are sensed, and the weighted sum of the output voltages is fed back to modulate the duty cycle, *d*. Compared with the conventional single-output-sensing feedback control, the WVMC redistributes the dc regulation error among the sensed outputs [9]. If the weighting factors and the compensator are properly designed, the dc cross-regulation and dynamic characteristics of the sensed outputs can be significantly improved.

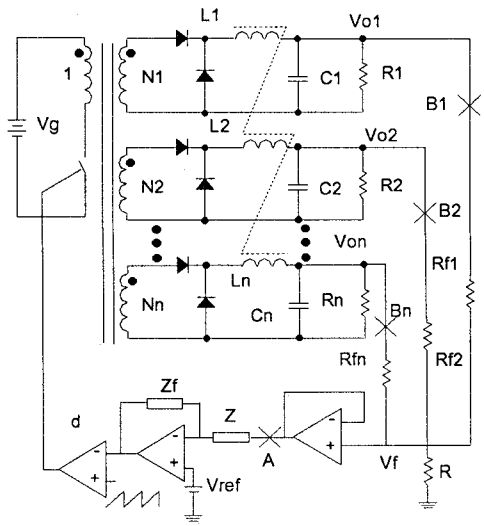

Fig. 1. A multiple-output forward converter with weighted voltage-mode control and coupled output filter inductors.

Generally, the small-signal properties of a multiple-output converter with WVMC are quite different from those of a single-output converter or a multiple-output converter with only one regulated output. The differences are primarily caused by interaction among the outputs of the converter with WVMC, resulting higher order of the small-signal transfer functions. For a multiple-output forward converter with WVMC, the order of the small-signal transfer functions is *2n*, where *n* is the number of the sensed outputs. Furthermore, when WVMC is used simultaneously with the coupled output-filter inductors, the positions of poles and zeros of the small-signal transfer functions are significantly altered compared with the non-coupled case. As a result, the loop compensation design for WVMC is different from that of the conventional single-output-sensed feedback control.

This work has been supported in part by Delta Electronic Ind. Co., Ltd., Taiwan, and the Virginia Center for Innovative Technology.

0-7803-1243-0/93$03.00 © 1993 IEEE

The dc analysis of the WVMC and the design procedure for determining the weighing factors for a multiple-output forward converter were presented in [9]. The purpose of this study is to present a design-oriented ac analysis for the same converter.

In Section II, a complete small-signal model of a forward converter with n outputs is derived using the pulse-width-modulation (PWM) switch modeling approach [10]. The model is derived by assuming the most general case with coupled output-filter inductors. Section III discusses the effects of weighting factors and coupling coefficients on the system characteristics. The design considerations are discussed in Section IV. Finally, a design example and experimental results that verify the derived model and the proposed design procedure are given in Section V. Key results are summarized in Section VI.

It should be noted that although only the analysis and design of a forward converter are presented in this paper, the same approach can be easily extended to any other multiple-output topology with WVMC.

II. SMALL-SIGNAL MODELING

The small-signal model is obtained by applying PWM-switch modeling techniques [10]. In this technique, the nonlinear PWM switches of a converter are replaced with a simple linear small-signal circuit. Figure 2 shows the small-signal equivalent circuit of a multiple-output converter with coupled inductors obtained by replacing the active and passive switches with the small-signal model. To simplify the analysis, the following assumptions are made:

1) All the switches are ideal, *i.e.*, they have zero on-resistances and junction capacitances, and infinite off-resistances.
2) The transformer is ideal, *i.e.*, the magnetizing inductance is infinite, and the leakage inductances are zero. The core and winding losses are negligible.
3) The output filter inductors do not have any core loss.

It should be emphasized that these assumptions are only justified for small-signal analysis because the circuit parasitics have negligible effect on the ac characteristics. However, the same parasitics have significant effects on the dc characteristics and cannot be neglected in the dc analysis as discussed in [1,2,3,6,7,9].

The small signal model is derived for the operation in continuous conduction mode (CCM). The state space variables are defined as the inductor currents and capacitor voltages:

$$X=\left[i_{L1}\quad i_{L2}\quad \cdots\quad i_{Ln}\quad v_{c1}\quad v_{c2}\quad \cdots\quad v_{cn}\right]^{T}_{2n\times 1}, \tag{1}$$

the input variables are the input voltage, load currents and duty cycle:

$$U=\left[v_{in}\quad d\quad i_{o1}\quad i_{o2}\quad \cdots\quad i_{on}\right]^{T}_{(n+2)\times 1}, \tag{2}$$

and the output variables are the output voltages:

$$Y=\left[v_{o1}\quad v_{o2}\quad \cdots\quad v_{on}\right]^{T}_{n\times 1}. \tag{3}$$

The resulting state equations are

$$\dot{X}=AX+BU, \tag{4}$$

$$Y=CX+DU, \tag{5}$$

where

$$A=\begin{bmatrix}-M^{-1}P\\ S\end{bmatrix}_{2n\times 2n}, \tag{6}$$

$$B=\begin{bmatrix}M^{-1}R\\ T\end{bmatrix}_{2n\times(n+2)}, \tag{7}$$

$$C=\begin{bmatrix}R_{p1} & 0 & \cdots & 0 & R_{q1} & 0 & \cdots & 0\\ 0 & R_{p2} & \cdots & 0 & 0 & R_{q2} & \cdots & 0\\ \vdots & \vdots & \ddots & \vdots & \vdots & \vdots & \ddots & \vdots\\ 0 & 0 & \cdots & R_{pn} & 0 & 0 & \cdots & R_{qn}\end{bmatrix}_{n\times 2n}, \tag{8}$$

$$D=\begin{bmatrix}0 & 0 & R_{p1} & 0 & \cdots & 0\\ 0 & 0 & 0 & R_{p2} & \cdots & 0\\ \vdots & \vdots & \vdots & \vdots & \ddots & \vdots\\ 0 & 0 & 0 & 0 & \cdots & R_{pn}\end{bmatrix}_{n\times(n+2)} \tag{9}$$

M is the inductance matrix which is defined as:

$$M=\begin{bmatrix}M_{11} & M_{12} & \cdots & M_{1n}\\ M_{21} & M_{22} & \cdots & M_{2n}\\ \vdots & \vdots & \ddots & \vdots\\ M_{n1} & M_{n2} & \cdots & M_{nn}\end{bmatrix}_{n\times n}, \tag{10}$$

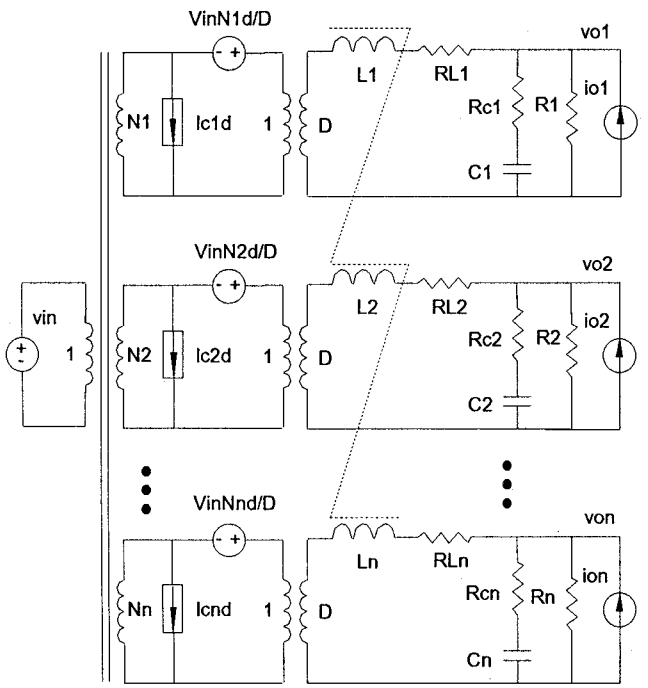

Fig. 2. Small-signal circuit model obtained by using PWM switch model.

$$P=\begin{bmatrix} R_{t1} & 0 & \cdots & 0 & R_{q1} & 0 & \cdots & 0 \\ 0 & R_{t2} & \cdots & 0 & 0 & R_{q2} & \cdots & 0 \\ \vdots & \vdots & \ddots & \vdots & \vdots & \vdots & \ddots & \vdots \\ 0 & 0 & \cdots & R_{tn} & 0 & 0 & \cdots & Rqn \end{bmatrix}_{n\times 2n}, \quad (11)$$

$$R=\begin{bmatrix} N_1V_{in} & N_1D & -R_{p1} & 0 & \cdots & 0 \\ N_2V_{in} & N_2D & 0 & -R_{p2} & \cdots & 0 \\ \vdots & \vdots & \vdots & \vdots & \ddots & \vdots \\ N_nV_{in} & N_nD & 0 & 0 & \cdots & -R_{pn} \end{bmatrix}_{n\times(n+2)}, \quad (12)$$

$$S=\begin{bmatrix} \frac{R_1}{\tau_1} & 0 & \cdots & 0 & -\frac{1}{\tau_1} & 0 & \cdots & 0 \\ 0 & \frac{R_2}{\tau_2} & \cdots & 0 & 0 & -\frac{1}{\tau_2} & \cdots & 0 \\ \vdots & \vdots & \ddots & \vdots & \vdots & \vdots & \ddots & \vdots \\ 0 & 0 & \cdots & \frac{R_n}{\tau_n} & 0 & 0 & \cdots & -\frac{1}{\tau_n} \end{bmatrix}_{n\times 2n}, \quad (13)$$

$$T=\begin{bmatrix} 0 & 0 & \frac{R_1}{\tau_1} & 0 & \cdots & 0 \\ 0 & 0 & 0 & \frac{R_2}{\tau_2} & \cdots & 0 \\ \vdots & \vdots & \vdots & \vdots & \ddots & \vdots \\ 0 & 0 & 0 & 0 & \cdots & \frac{R_n}{\tau_n} \end{bmatrix}_{n\times(n+2)}, \quad (14)$$

where the elements of the coefficient matrices are defined as:

$$M_{ij}=k_{ij}\sqrt{L_iL_j},\ i\neq j,\quad M_{ii}=L_i,$$

$$R_{pi}=R_i//R_{ci},\quad R_{qi}=\frac{R_i}{R_i+R_{ci}},$$

$$R_{ti}=R_{Li}+R_i//R_{ci},\quad \tau_i=(R_i+R_{ci})C_i,\quad (i,j=1,\ldots n),$$

and k_{ij} is the coupling coefficient between the i-th and j-th output filter inductors, R_i the load resistor, C_i the filter capacitor, R_{ci} the equivalent series resistor (ESR) of the capacitor, and N_i the transformer turns ratio.

Equations (1) through (14) are general expressions which describe the small-signal behavior of a forward converter with n outputs in time domain. The system characteristics in the frequency domain, where design and measurements are usually performed, are easily obtained by taking Laplace transform of the state equation.

III. EFFECTS OF WEIGHTED VOLTAGE-MODE CONTROL AND COUPLED INDUCTORS

In this section, the individual as well as the combined effects of the weighting factors and coupling coefficients of the output filter inductors on small-signal transfer function are investigated. First, the effects of the weighting factors are studied by assuming no coupling between the output filter inductors. Then the effects of the coupling coefficients in the absence of WVMC are studied. Finally, the combined effects of the weighting factors and coupling coefficients are discussed. To avoid lengthy expressions without losing generality, the following analysis is performed on a forward converter with two outputs.

A. Effects of Weighting Factors

To investigate the effects of weighting factors alone, it is assumed that the coupling coefficients are zero, *i.e.*, $k_{ij}=0$, $i,j=1,2$, $i\neq j$, in the small-signal model derived in the previous section. For WVMC, according to Fig. 1, the feedback signal, v_f, is derived from the weighted sum of the output voltages, *i.e.*:

$$v_f=K_1v_{o1}+K_2v_{o2}. \quad (15)$$

where K_1 and K_2 are the weighting factors which can be calculated from the weighting network resistors [9]:

$$K_1=\frac{R_{f2}R}{R_{f1}R_{f2}+R_{f1}R+R_{f2}R},K_2=\frac{R_{f1}R}{R_{f1}R_{f2}+R_{f1}R+R_{f2}R}, \quad (16)$$

From Eqs. (1) - (16), the control-to-feedback transfer function is derived as:

$$G_{vd}(s)=\frac{v_f}{d}=\frac{K_1N_1V_{in}(1+\frac{s}{s_{z1}})}{(1+\frac{s}{\omega_{o1}Q_1}+\frac{s^2}{\omega_{o1}^2})}+\frac{K_2N_2V_{in}(1+\frac{s}{s_{z2}})}{(1+\frac{s}{\omega_{o2}Q_2}+\frac{s^2}{\omega_{o2}^2})} \quad (17)$$

where ω_{oi} is the resonant frequency of each output filter, Q_i the damping coefficient, and s_{zi} the ESR zero. They are given by:

$$\omega_{oi}=\frac{1}{\sqrt{L_iC_i}}, \quad (18)$$

$$Q_i=\frac{1}{\omega_{oi}}\frac{1}{L_i/(R_{Li}+R_i)+C_i(R_{ci}+R_{Li}//R_i)}, \quad (19)$$

$$s_{zi}=1/(R_{ci}C_i),\quad i=1,2. \quad (20)$$

Assuming that the frequencies of the ESR zeros are much higher than those of the power stage poles, the control-to-feedback transfer function can be rewritten into the pole-zero form:

$$G_{vd}(s)=V_{in}\frac{K_B(1+\frac{s}{s_z})(1+\frac{s}{\omega_zQ_z}+\frac{s^2}{\omega_z^2})}{(1+\frac{s}{\omega_{o1}Q_1}+\frac{s^2}{\omega_{o1}^2})(1+\frac{s}{\omega_{o2}Q_2}+\frac{s^2}{\omega_{o2}^2})}, \quad (21)$$

where

$$K_B=K_1N_1+K_2N_2, \quad (22)$$

$$\frac{1}{s_z}\approx\frac{1}{K_1N_1+K_2N_2}(\frac{K_1N_1}{s_{z1}}+\frac{K_2N_2}{s_{z2}}), \quad (23)$$

$$\frac{1}{\omega_z^2}\approx\frac{1}{K_1N_1+K_2N_2}(\frac{K_1N_1}{\omega_{o1}^2}+\frac{K_2N_2}{\omega_{o2}^2}). \quad (24)$$

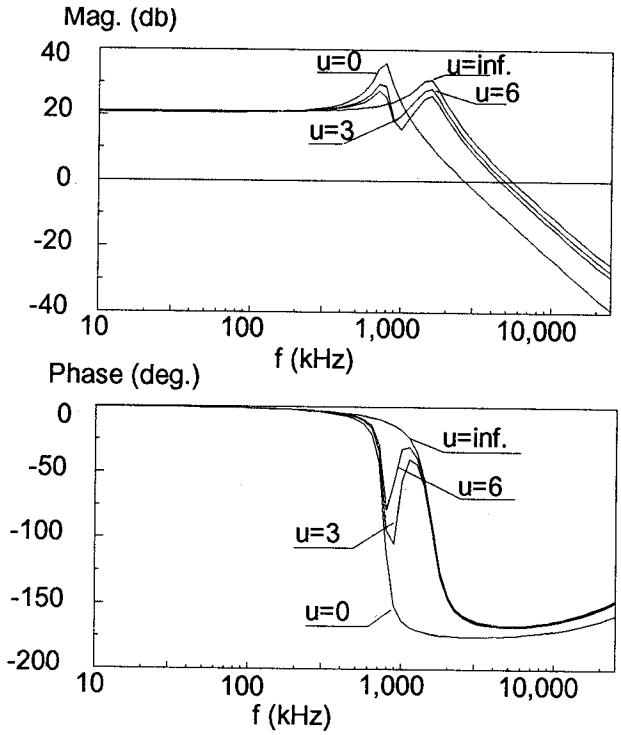

Fig. 3. Bode plot of control-to-feedback (v_f /d) transfer function of a multiple-output converter with WVMC. The ratio of the weighting factors is the running parameter.

As can be seen from Eq. (21), unlike the two-output converter with single-output feedback control where the transfer function is of 2nd order, the transfer function of the same converter with WVMC becomes 4th order. Figure 3 shows the Bode plot of the control-to-feedback transfer function (v_f /d) using the ratio of the weighting factors, $u(=K1/K2)$, as running parameter. According to Eq. (21), the transfer function has two pairs of complex poles, one pair of complex zeros, and a real zero (equivalent ESR zero). From Eq. (18), resonant frequencies ω_{o1} and ω_{o2} of the complex poles do not depend on the weighting factors. However, the resonant frequency of complex zero, ω_z, and the real zero, s_z, are the functions of weighting factors K_1 and K_2 as can be seen from Eqs. (23) and (24). Therefore, as the ratio of the weighting factors varies, the positions of the poles are fixed, and the positions of the zeros are changing. From Eq. (24), it can be shown that no matter how the zeros move, the poles and zeros are always interlaced, *i.e.*:

$$\omega_{o1} \le \omega_z \le \omega_{o2}, \tag{25}$$

assuming $\omega_{o1} \le \omega_{o2}$.

The interlaced pole-zero distribution makes the system behavior at both low and high frequencies similar to that of a 2nd order system. In the middle frequency range, however, the frequency characteristics exhibits multiple peaks. When designing the compensator, the crossover of the loop gain should be chosen away from this range to prevent conditional stability.

If the extreme case is assumed, *i.e.*, $u = 0$ (or ∞), the transfer function is reduced to a 2nd order system. Therefore the single feedback control scheme is a special case of the weighted voltage-mode control.

B. Effects of Coupled Inductors

The control-to-output transfer functions of the two-output converter with coupled inductors but without WVMC is derived as following:

$$G_{vd1} = \frac{v_{o1}}{d} = \frac{\begin{array}{l} V_{in}(1+R_{C1}C_1 s)\{N_1[1+(R_{C2}C_2+\frac{L_2}{R_2} \\ +R_{L2}C_2)s+L_2C_2s^2]-N_2[\frac{M_{12}}{R_2}s+C_2M_{12}s^2]\} \end{array}}{\begin{array}{l} [1+(R_{C1}C_1+\frac{L_1}{R_1}+R_{L1}C_1)s+L_1C_1)s^2] \\ [1+(R_{C2}C_2+\frac{L_2}{R_2}+R_{L2}C_2)s+L_2C_2)s^2] \\ -[\frac{M_{12}}{R_1}s+C_1M_{12}s^2][\frac{M_{12}}{R_2}s+C_2M_{12}s^2] \end{array}} \cdot \tag{26}$$

Exchanging the subscript 1 (or 2) to 2 (or 1), the control-to-output-2 transfer function, G_{vd2}, can be obtained. Obviously, if there is no coupling between the output inductors L_1 and L_2, *i.e.*, the coupling coefficient $K=k_{12}=0$, the transfer function reduces to that of the single output converter, which is a 2nd order system.

Figure 4 shows the control-to-output transfer functions for both outputs, where the coupling coefficient K is the running parameter. Generally, the transfer functions are of 4th order, with two pairs of complex poles, a pair of complex zeros, and a real zero. The resonant frequencies of both poles and zeros depend on the value of the coupling coefficient. Unlike the case of WVMC where the poles and zeros are always interlaced, here the control-to-output transfer function for one output has an interlaced pole-zero distribution (Fig. 4(a)), whereas another has a non-interlaced pole-zero distribution (Fig. 4 (b)). As a result, for the conventional single-output feedback control, the loop compensation is dependent on the choice of the sensed output. It is more desirable to feedback the output whose control-to-output transfer function has interlaced poles and zeros.

C. Combined Effects of WVMC and Coupled Inductors

When WVMC and coupled inductors are employed simultaneously, the control-to-feedback transfer function is obtained by summing two weighted outputs:

$$\frac{v_f}{d} = K_1 G_{vd1} + K_2 G_{vd2}. \tag{27}$$

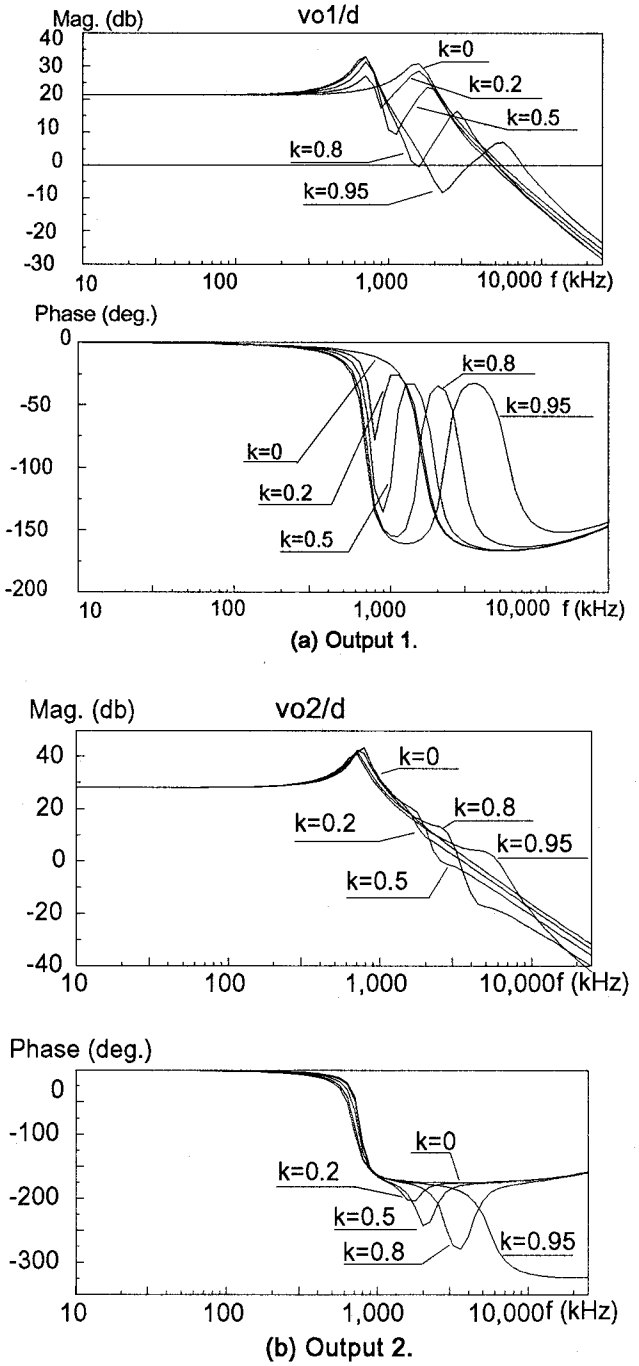

Fig. 4. Bode plots of control-to-output transfer function of the dual-output forward converter with coupled inductors: (a) output 1; (b) output 2. The coupling coefficient is the running parameter.

where G_{vd1} and G_{vd2} are defined by Eq. (26).

Figure 5 shows the Bode plot of the control-to-feedback transfer function. For different ratio of the weighting factors and different coupling coefficient, the system behavior can change drastically, from 2nd order system to 4th order system, from an interlaced pole-zero distribution to a non-interlaced distribution.

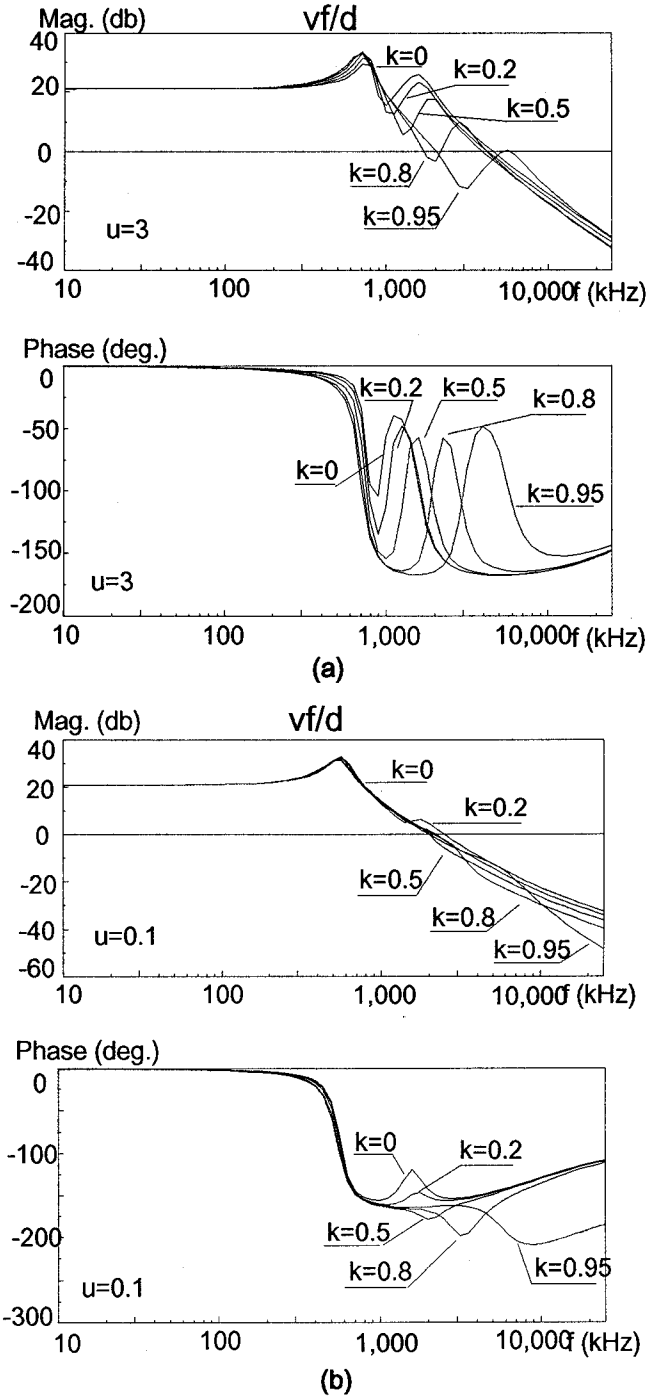

Fig. 5. Bode plots of control-to-feedback (v_f /d) transfer function of the dual-output converter with WVMC and coupled inductors for different weighting factors: (a) $u=K_1/K_2=3$; (b) $u=K_1/K_2=0.1$. The coupling coefficient, K, is the running parameter.

Figure 6 shows the pole-zero distribution for different values of the coupling coefficient and the ratio of the weighting factors where the resonant frequencies of the output filter are not close to each other. As can be seen, the locations of the complex zeros are dependent on both the

ratio of the weighting factors and the coupling coefficient, whereas the locations of the complex poles are only affected by coupling coefficient. Furthermore, if the resonant frequencies of the two output filters are separated, the low-frequency complex poles are relatively fixed. Then the system transfer function can be written into pole-zero form:

$$G_{vd}(s)=\frac{V_{in}K_B(1+\frac{s}{s_{zt}})(1+\frac{s}{\omega_{zt}Q_{zt}}+\frac{s^2}{\omega_{zt}^2})}{(1+\frac{s}{\omega_{pt1}Q_{pt1}}+\frac{s^2}{\omega_{pt1}^2})(1+\frac{s}{\omega_{pt2}Q_{pt2}}+\frac{s^2}{\omega_{pt2}^2})}. \quad (28)$$

where

$$K_B=K_1N_1+K_2N_2, \quad (29)$$

and the poles and zeros are approximated as:

$$s_{zt}\approx\frac{K_1N_1+K_2N_2}{K_1N_1R_{c1}C_1+K_2N_2R_{c2}C_2}, \quad (30)$$

$$\omega_{zt}^2\approx\frac{K_1N_1+K_2N_2}{(1-K)(K_1N_1L_2C_2+K_2N_2L_1C_1)}, \quad (31)$$

$$\omega_{pt1}^2\approx\frac{1}{\max(L_2C_2,L_1C_1)}, \text{ and} \quad (32)$$

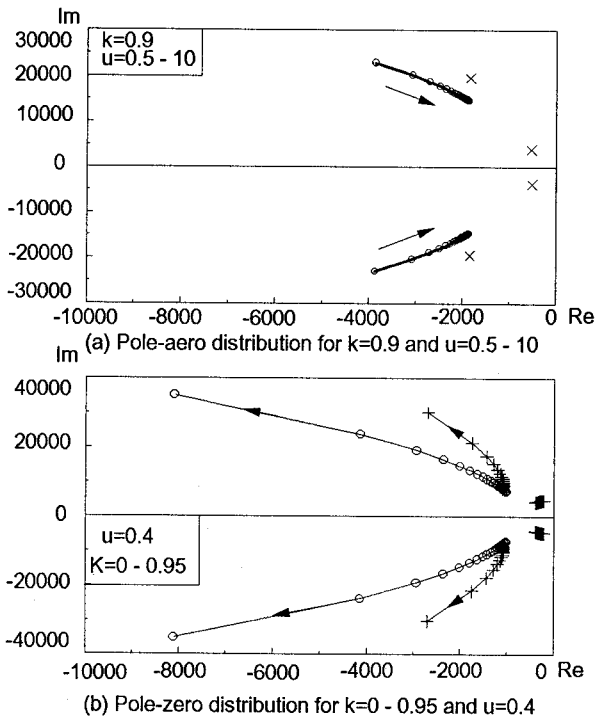

Fig. 6. Pole-zero distribution of a multiple-output converter with the weighted voltage-mode control and coupled inductors for different values of the weighting factors and the coupling coefficient. The equivalent real zero locates far beyond the left boundary, and is not shown here. (a) *K=0.9, u=0.5 - 10*; (b) *k=0 - 0.95, u=0.4*.

$$\omega_{pt2}^2\approx\frac{1}{(1-K^2)\min(L_1C_1,L_2C_2)}. \quad (33)$$

IV. DESIGN CONSIDERATIONS

It can be seen that, from the above analyses, the system transfer functions fall into two categories: (1) those with interlaced complex poles and zeros, and (2) those with non-interlaced poles and zeros. The converter with WVMC belongs only to category (1). For the converter with coupled inductors only, one control-to-output transfer function falls into (1), and the other transfer function falls into (2). As for the converter with both WVMC and coupled inductor, the transfer function can be either type, depending on the converter parameters, coupling coefficient, and weighting factors. In this section, the compensator design for different cases is discussed.

A. Compensator Design for the System With Interlaced Complex Poles and Zeros

For a converter whose control-to-feedback transfer function has interlaced complex poles and zeros, the system behavior at both low and high frequencies is similar to that of the single output converter. The major difference is in the middle frequency range where the characteristics show multiple peaks, as can be seen in Figs. 3, 4(a) and 5(a). No matter how the poles and zeros move, the phase never exceeds -180°. As a result, the commonly used compensator with an integrator plus two poles and two zeros:

$$A_c(s)=\frac{K_I}{s}\frac{(s+s_{zc1})(s+s_{zc2})}{(s+s_{pc1})(s+s_{pc2})}, \quad (34)$$

can be employed. The design of the integrator gain and compensator poles are similar to the design for the single output converter [11]. The first pole is placed to cancel the equivalent ESR zero. The second pole is placed at approximately one half of the switching frequency to attenuate the switching noise in the modulator. The control bandwidth and stability margin are determined by the placement of the compensator zeros. To achieve a fast response, the first zero is placed slightly below the low frequency complex pole $s_{zc1}\le\omega_{pt1}$. The position of the second zero determines the control bandwidth and stability margin. Figure 7 shows the loop gain with two different zero placements. It can be seen that both designs give about same phase margin. But checking the crossover of the loop gain, it shows that the design with the second zero after the complex zero of the plant yields a lower crossover frequency due to the peaking of the complex zero. Therefore, it is suggested that the second compensator zero be chosen as

$$\omega_{pt1}\le s_{zc2}\le\omega_{zt} \quad (35)$$

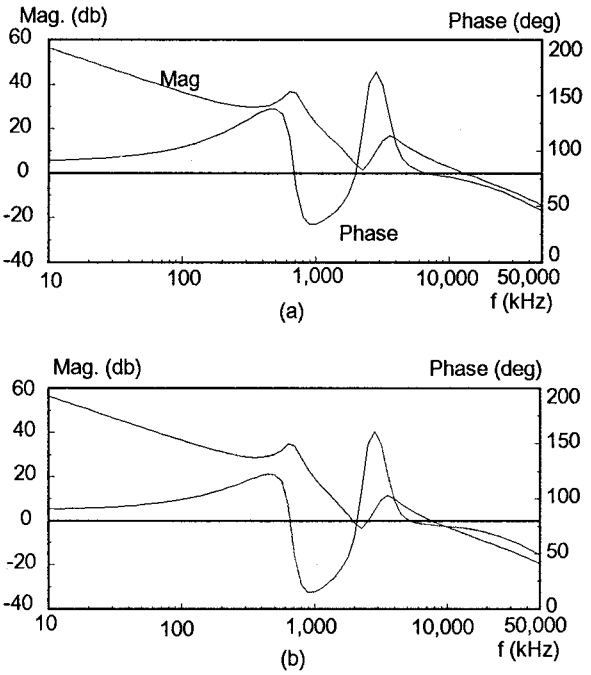

Fig. 7. Loop gain of the multiple-output converter with WVMC and coupled inductors for different values of the second zero: (a) $f_{z2}=f_{o1}$; (b) $f_{z2}=2f_{o1}$. The right axes are phase margin.

B. Compensator Design for System With Non-Interlaced Poles and Zeros

For a converter whose transfer function has non-interlaced poles and zeros, the phase delay can exceed -180° because of two pairs consecutive complex poles, as shown in Figs. 4(b), 5(b). If the second pair of complex poles is followed immediately by a pair of complex zeros, excessive phase delay will not occur. Therefore the previously discussed 2-zero-3-pole compensator still can be used. However, if the second pair complex poles and the complex zeros are widely separated and the phase delay exceeds -270°, the system crossover frequency has to be chosen below the resonant frequency of the first pair of complex poles. In this case, a single integrator with a relatively low gain is suitable for the compensator. Apparently, the closed-loop performance of the converter with noninterlaced poles and zeros is inferior to that of the converter with interlaced poles and zeros.

C. Power Stage Design Consideration

From above discussion, it is obvious that a system with interlaced complex poles and zeros is more desirable than a system with non-interlaced poles and zero. Since the positions of the poles and zeros of the power stage control-to-feedback transfer function are dependent on the coupling coefficient and the weighting factors, the degree of coupling can be adjusted so that the control-to-feedback transfer function has interlaced poles and zeros.

Equations (31) - (33) give the approximated expressions for the resonant frequencies of the complex poles and zeros. To make the complex poles and zeros interlace:

$$\omega_{pt1}^2 \le \omega_{zc}^2 \le \omega_{pt2}^2. \tag{36}$$

The left side of the inequality is always met, to meet right side of the inequality, there must be

$$\frac{K_1N_1+K_2N_2}{(1-K)(K_1N_1L_2C_2+K_2N_2L_1C_1)} \le \frac{1}{(1-K^2)\min(L_1C_1,L_2C_2)}, \tag{37}$$

or the coupling coefficient should meet:

$$K \le \frac{uN_1L_2C_2+N_2L_1C_1}{(uN_1+N_2)\min(L_1C_1,L_2C_2)} - 1. \tag{38}$$

From Eq. (38), it can be seen that a large coupling coefficient tends to yield a noninterlaced pole-zero distribution, and the system tends to have less stability margin for the same compensator design, which agrees with the finding reported in [8].

V. DESIGN EXAMPLE

In this section, the design of a dual-output forward converter is illustrated. The design specifications of the converter are [9]:

- input line voltage V_{in}, $170\ V$ - $270\ V$,
- 5 V output: $4.8V \le V_{o1} \le 5.2V$, $2A \le I_{o1} \le 15A$, and
- 12 V output: $11.5V \le V_{o2} \le 12.7V$, $0.5A \le I_{o2} \le 3A$.

The experimental dual-output forward converter operating at 100 kHz was built with its circuit parameters as shown in Table 1.

To meet dc regulation specification, the ratio of the weighting factors is chosen as $u=K_1/K_2=3$, as explained in [9], which yields $K_1=0.567$, $K_2=0.189$.

The turns ratio of the coupled inductors is equal to the ratio of the output voltages [5]. The coupling between the output inductors is designed $K=0.95$.

Using Eqs. (31) - (33) derived in Section III, the values of the complex poles and zeros are

$$\omega_{zt} \approx 25291.78 \quad rad/s, \tag{39}$$

$$\omega_{pt1} \approx 4809.5 \quad rad/s, \tag{40}$$

$$\omega_{pt2} \approx 266548.2 \quad rad/s. \tag{41}$$

Table 1. List of the Circuit Parameters.

N_1	0.067	N_2	0.156
L_1 (μH)	69	R_{L1} (Ω)	0.037
L_2 (μH)	378	R_{L2} (Ω)	0.12
C_1 (μF)	210	R_{c1}(Ω)	0.023
C_2 (μF)	114	R_{c2}(Ω)	0.0057
R_{1max} (Ω)	2.5	R_{2max} (Ω)	24

Since the complex poles and zeros are interlaced, the compensator with an integrator plus two poles and two zeros, Eq. (34), is employed. The first pole is placed at the equivalent ESR zero:

$$\omega_{pc1} \approx 285017.8 \quad rad/s. \tag{42}$$

The second pole is placed at the half of the switching frequency:

$$\omega_{pc2} \approx 314159.3 \quad rad/s. \tag{43}$$

The two zeros are placed at the first complex pole:

$$\omega_{pc1} \approx \omega_{pc2} \approx \omega_{pt1} \approx 4809.5 \quad rad/s. \tag{44}$$

The system loop gain is measured at the feedback path after the summing junction point A as shown in Fig. 8. The system has a phase margin of 75°. The calculations agree well with the measurements except when frequency approaches half of the switching frequency.

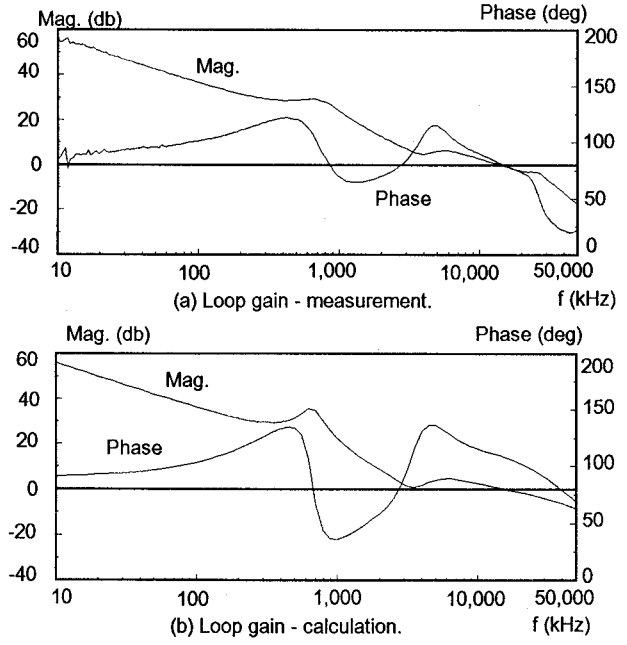

Fig. 8. Loop gain measurement of the dual-output forward converter with WVMC. The right axes are phase margin.

VI. SUMMARY

A small-signal model for a multiple-output forward converter with weighted voltage-mode control is derived. The converter control-to-feedback transfer function is of $2n^{th}$ order. For different values of the weighting factors and the coupling coefficient of the output filter inductors, the system small-signal behavior can vary from the desired interlaced pole-zero distribution to non-interlaced pole-zero distribution. The system with interlaced poles and zeros is easier to compensate and possesses a relatively larger stability margin. The analytical model indicates that by adjusting the values of the weighting factors and the coupling coefficient of the output inductors according to Eq. (38), the interlaced pole-zero pattern can be obtained.

For a system with interlaced complex poles and zeros, a design employing the compensator with 2 zeros and 3 poles can be used to yield satisfactory performance and stability margin. For a system with non-interlaced complex poles and zeros, an integrator with relatively low gain is recommended to provide a loop crossover prior to the first double pole in order to provide adequate stability margin. In this case, the cross-over of the loop gain is significantly reduced compared to the previous design.

VII. REFERENCES

[1] T. G. Wilson, Jr., "Cross Regulation in an Energy-Storage DC-to-DC Converter with Two Regulated Outputs," *IEEE Power Electronics Specialists Conf. Rec.*, 1977, pp. 190-199.

[2] T. G. Wilson, Jr., "Cross Regulation in a Two-Output DC-to-DC Converter with Application to Testing of Energy-Storage Transformer," *IEEE Power Electronics Specialists Conf. Rec.*, 1978, pp. 124-134.

[3] K. Harada, T. Nabeshima, and K. Hisanaga, "State-Space Analysis of the Cross-Regulation," *IEEE Power Electronics Specialists Conf. Rec.*, 1979, pp. 186-192.

[4] S. Cuk and R. D. Middlebrook, "Coupled-Inductor and Other Extensions of a New Optimum Topology Switching DC-to-DC Converter," *Advances in Switched-Mode Power Conversion*, Vols. I and II, 1983, pp. 331 - 347.

[5] L. H. Dixon, Jr., "Coupled Filter Inductors in Multiple Output Buck Regulators Provide Dramatic Performance Improvement," *Unitrode Power Supply Design Seminar Book*, 1988, pp. M7-1- 7-10.

[6] H. Matsuo, "Comparison of Multiple-Output DC-DC Converters Using Cross Regulation," *IEEE Power Electronics Specialists Conf. Rec.*, 1979, pp. 169-185.

[7] F. Kurokawa and H. Matsuo, "A New Multiple-Output Hybrid Power Supply," *IEEE Trans. Power Electronics*, vol. 3, no. 4, pp. 412-419, 1988.

[8] C.C. Liu, K.H. Ding, J.R. Young, and J.F. Beutler, "A Systematic Method for the Stability Analysis of Multiple-Output Converters," *IEEE Trans. Power Electronics*, vol. 2, no. 4, pp. 343-353, 1989.

[9] Q. Chen, F.C. Lee, and M.M. Jovanović, "DC Analysis and Design of Multiple-Output Forward Converters with Weighted Voltage-Mode Control," *Proc. IEEE Applied Power Electronics Conf.*, March 1993.

[10] V. Vorperian, "Simplified Analysis of PWM Converters Using the Model of the PWM Switch: Parts I and II," *IEEE Trans. on Aerospace and Electronic Systems*, vol. 26, no. 3, pp 490-505, 1990.

[11] D.M. Sable, R. Ridley, B.H. Cho, "Comparison of Performance of Single-Loop and Current-Injection Control for PWM Converters that Operate in Both Continuous and Discontinuous Modes of Operation," *IEEE Trans. Power Electronics*, vol. 7, no. 1, pp. 136-142, 1992.